CrossMark

Inhomogeneous Phase Effect of Smart Meta-Superconducting MgB$_2$

Yongbo Li[1] · **Honggang Chen**[1] · **Weichang Qi**[1] ·
Guowei Chen[1] · **Xiaopeng Zhao**[1]

Abstract The inhomogeneous phase of a smart meta-superconductor has a great effect on its superconductivity. In this paper, the effect of concentration, dimensions, electroluminescence (EL) intensity, and distribution of the inhomogeneous phase on the superconducting critical temperature (T_C) has been systematically investigated. An ex situ solid sintering was utilized to prepare smart meta-superconducting MgB$_2$ doped with six kinds of electroluminescent materials, such as YVO$_4$:Eu^{3+} and Y$_2$O$_3$:Eu^{3+} flakes. Elemental mappings through energy dispersive spectroscopy (EDS) show that the inhomogeneous phase is comparatively uniformly dispersed around the MgB$_2$ particles; thus V, Y, and Eu were accumulated at a small area. The measurement results show that the optimum doping concentration of the meta-superconducting MgB$_2$ is 2.0 wt%. The offset temperature (T_C^{off}) of the sample doped with 2.0 wt% dopant A is 1.6 K higher than that of pure MgB$_2$. The improvement in T_C^{off} is likely related to the sizes, thickness, and EL intensity of the inhomogeneous phase of MgB$_2$ smart meta-superconductor. This experiment provides a novel approach to enhance T_C.

Keywords Smart meta-superconductor · Inhomogeneous phase · MgB$_2$ ·
Ex situ sintering · T_C

1 Introduction

The superconductivity of MgB$_2$ was first discovered in 2001 [1]. MgB$_2$ is a promising material with large-scale applications because of its simple crystal structure, high

---

✉ Xiaopeng Zhao
xpzhao@nwpu.edu.cn

1   Smart Materials Laboratory, Department of Applied Physics,
     Northwestern Polytechnical University, Xi'an 710129, People's Republic of China

T_C (39.0 K), large coherence lengths, and high critical current densities and fields [2]. Various methods have been proposed to improve T_C of MgB_2. One of the most important methods is chemical doping. Al and C are considered useful elements for effective substitutional doping in MgB_2. However, partially substituting Mg with Al or B with C decreases T_C of MgB_2 [3–7]. A high doping content even causes the loss of superconductivity. It is generally considered that the decrease in T_C is caused by the large electron concentration [8,9]. Thus, researchers have tried to improve the T_C by increasing the density of hole carriers by substituting Mg with Li. However, the results of this method are unsatisfactory [10,11]. The crystal lattice of MgB_2 is distorted during the substitutional doping process. In non-substitutional doping, a dopant, which acts as an impurity phase, is present in the grain boundary of MgB_2. This condition decreases grain connectivity and increases impurity scattering [12–14]. As such, effective methods should be developed to improve T_C of MgB_2.

Chemical doping, which can increase the pinning force, can also be applied to improve the critical current density of MgB_2. Significant progress has been made in this regard [15,16]. However, practical applications of MgB_2 have yet to be implemented. First, chemical doping generally involves the direct mixing of a raw material (B and Mg) with a dopant. This dopant may react with B or Mg during subsequent experimental processes. Second, a B-rich phase may form during the in situ solid sintering because the melting point of Mg is relatively low and Mg vapor forms in this stage. Thus, excessive Mg is added during MgB_2 preparation, especially in large-scale production, which leads to the formation of residual Mg in the final product. Dopant and residual Mg greatly decrease the superconducting transition temperature and increase the transition width [17–22]. In order to make a material in the superconducting state during practical applications, we should set a temperature lower than the offset temperature of the material. Therefore, many difficulties impede the practical applications of MgB_2 even though its critical current density is large.

Meta-materials are a type of composite materials with artificial structures that can provide special functions that are absent in nature [23–25]. Researchers have started to try to improve T_C via the meta-material method. In 2007, our group proposed that doping electroluminescent materials into a superconducting material to form a smart meta-superconductor may be an effective method to improve T_C [26,27]. Zhang et al. [28] prepared MgB_2 doped with an efficient electroluminescent material Y_2O_3:Eu^{3+} by an in situ solid sintering process. Tao et al. [29] prepared MgB_2 doped with Y_2O_3:Eu^{3+} via a modified ex situ process and confirmed that this method is favorable for T_C improvement. According to homogeneous system theory [30], Smolyaninov et al. proposed that a superconducting meta-material with an effective dielectric response function that is less and approximately equal to zero may exhibit high T_C [31], and they verified this theory in their subsequent experiments [32,33]. Meta-superconductor has attracted lots of concerns.

Based on our previous work, combining a superconductor and an inhomogeneous phase to form a smart meta-superconductor may be an effective method for T_C improvement. The results show that the concentration, dimensions, and distribution of the inhomogeneous phase all affect the critical temperature of the smart meta-superconductor. In order to systematically investigate the influence of inhomogeneous phase on the superconductivity, six kinds of dopants with different sizes were prepared
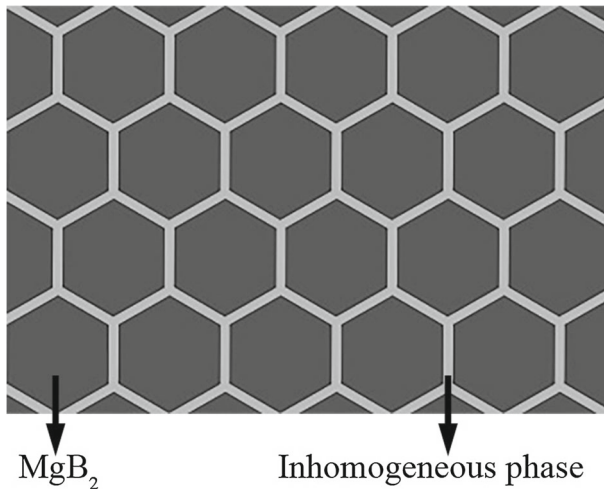
Fig. 1 Microstructure model of the smart meta-superconducting MgB_2 [29]

through a hydrothermal method in this study [34]. MgB_2 doped with these dopants were prepared via a modified ex situ solid sintering. Results indicate that these dopants display a limited effect on the onset temperature but elicit a remarkable influence on the offset temperature. Among these samples, the sample doped with 2.0 wt% dopant A yields the highest T_C^{off}, which is 1.6 K higher than that of pure MgB_2.

2 Model

Figure 1 shows the microstructure model of smart meta-superconducting MgB_2, which consists of MgB_2 matrix and the inhomogeneous phase such as the EL material YVO_4:Eu^{3+} or Y_2O_3:Eu^{3+}. The hexagons in this figure represent MgB_2 particles consisting of MgB_2 multi-grains. The inhomogeneous phase is dispersed around the MgB_2 particles, just like the gray area in this figure. The thickness of the inhomogeneous phase in the model must satisfy the coherence length conditions. In the present study, YVO_4:Eu^{3+} disperses around the MgB_2 particles to form a meta-structure. Adjusting the applied electric field to control the EL of YVO_4:Eu^{3+} or Y_2O_3:Eu^{3+} may alter T_C of this smart meta-superconductor.

3 Experiment

1. Preparation of the dopants

0.153 g of Y_2O_3 and 0.012 g of Eu_2O_3 were weighed and transferred to a beaker. Approximately 4 mL of concentrated nitric acid was then added to the beaker. A kind of white precursor was formed after heating the solution at 70 °C. Afterward, a certain quantity of the precursor was dissolved in 4 mL deionized water to form a transparent solution, which was designated as L1. Another solution, which was designated as L2,

Table 1 Corresponding experimental conditions and dimensions for different dopants

Dopant	A	B	C	D	E	F
Temperature (°C)	25	25	8	4	2	0
React time (h)	12	48	2	2	2	2
Length (μm)	1–2	2–3	∼ 0.8	∼ 0.6	∼ 0.5	∼ 0.4
Thickness (nm)	100	200	80	60	50	40

was prepared by dissolving 0.577 g of ammonium oxalate in 14 mL deionized water. Solution L1 was added dropwise to solution L2. A white precipitate then formed. After adding 0.221 g Na_3VO_4, the solution pH was adjusted to 9 by adding NaOH. Subsequently, the solution was transferred to a reaction kettle. A hydrothermal reaction then occurred at 160 °C and was allowed to proceed for a certain period of time to form a liquid with precipitates. After washing several times with deionized water and absolute ethanol, we can get a kind of yellow precipitate, which was sintered at 800 °C for 2 h to form the final YVO_4:Eu^{3+} flake. The size and the composition of the dopants would been altered by changing the temperature for doping L1 into L2 and adjusting the time for the hydrothermal reaction. We have synthesized six kinds of dopants designated as A–F. Table 1 shows the corresponding experimental conditions and dimensions for these dopants. The composition of dopant A and B is YVO_4:Eu^{3+}, and the composition of dopant C–F is Y_2O_3:Eu^{3+} [34].

2. Preparation of MgB_2-based superconductor

MgB_2 powder was purchased from Luoyang Tongrun Information Technology Co., Ltd, and its purity is 95%. The weights of MgB_2 and the dopant were calculated based on the content of the dopant. Then, MgB_2 and the dopant were, respectively, weighed and added into alcohol to form two suspensions, which were sonicated for 10 min. Afterward, the dopant was added dropwise to MgB_2. The resulting suspension was further sonicated for 20 min. The final suspension was transferred into a culture dish, which was then placed in a vacuum oven for 1 h at 60 °C to yield a black powder. Finally, the powder was pressed into a tablet and placed in a small tantalum container, which was annealed at 800 °C for 2 h in the high-purity argon atmosphere with no external pressure. Ten doping samples were prepared with varying dopant and doping concentrations. The samples were designed as S1, S2, S3, S4, S5, S6, S7, S8, S9, and S10. A pure MgB_2 sample, which was marked as S, was likewise produced via the ex situ process. To ensure the reliability of the experimental results, we synthesized more than three samples of different kinds of MgB_2. T_C^{off} of each sample was measured more than twice. The dopant and doping concentration of the different samples are listed in Table 2.

4 Results and Discussion

Figure 2a–f shows the scanning electron microscopy (SEM) images of dopants A–F, respectively. The composition of dopant A and B is YVO_4:Eu^{3+}, and the composition

Table 2 Dopant and doping concentration of all the samples

Sample	S	S1	S2	S3	S4	S5	S6	S7	S8	S9	S10
Dopant	None	A	A	A	A	A	B	C	D	E	F
Concentration (wt%)	0	0.5	1	1.5	2	3	2	2	2	2	2
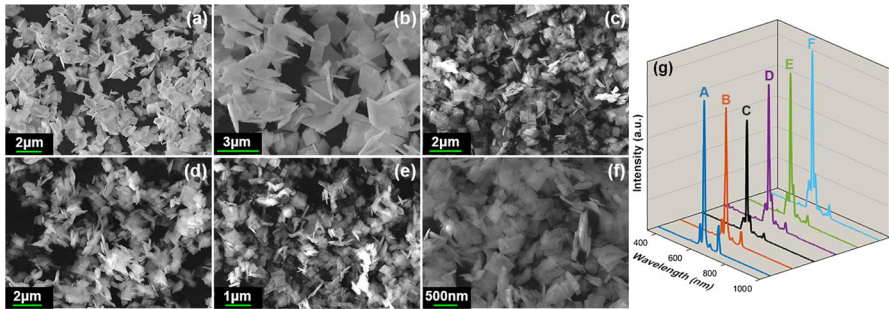
Fig. 2 SEM images (**a**–**f**) and EL spectra (**g**) of six kinds of dopants (Color figure online)
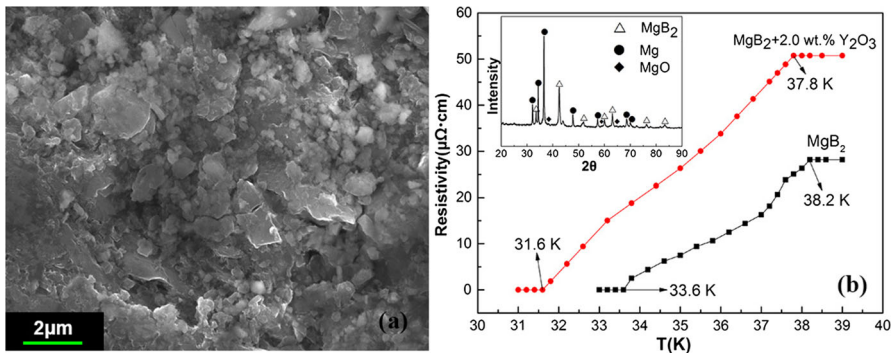

Fig. 3 **a** SEM image and **b** temperature-dependent resistivity curve of pure MgB_2 and MgB_2 doped with 2.0 wt% Y_2O_3. Inset: XRD spectrum of pure MgB_2 (Color figure online)

of dopant C–F is Y_2O_3:Eu^{3+}. It can be seen that all the dopants have square flake micromorphologies. Meanwhile, it can confirm that adjusting the doping temperature and the hydrothermal reaction time can change the dopant size. One dopant, however, does not have a strictly uniform flake structure. The size of dopant A is approximately 1–2 μm and that of dopant B is approximately 2–3 μm. The sizes of dopants C, D, E, and F are all under 1 μm, which decrease in turn. The difference in the sizes of these four dopants is not large. The thickness of these flakes is about one tenth of the length. Figure 2g shows the EL spectra of all the samples under the same excitation voltage. The EL intensities in order from the weak to the strong are: C, B, D, A, E, and F.

Figure 3a shows the SEM image of pure MgB_2. It can be seen that the size of pure MgB_2 particles is 0.2–2 μm with irregular micromorphology. There are obvious boundaries around the particles, which greatly enlarge the superconducting transition
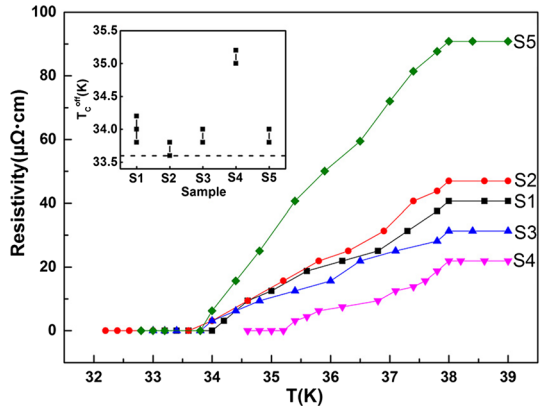
width ($\Delta T = 4.6$ K), as shown in Fig. 3b. Figure 3b presents the corresponding R–T
curve in a low-temperature range. The superconducting critical transition temperature
was determined by measuring the resistivity of the samples. The R–T curve was
measured using the four-probe method in a liquid helium cryogenic system made by
the Advanced Research Systems Company. Figure 3b shows that the onset (T_C^{on}) and
offset (T_C^{off}) critical temperatures of pure MgB$_2$ are 38.2 and 33.6 K, respectively.
The T_C is lower than the theoretical value and ΔT is larger than the theoretical value.
The inset of Fig. 3b is the X-ray diffraction (XRD) spectrum of the pure MgB$_2$.
The spectrum indicates that the main phases in the raw material are MgB$_2$ and Mg.
Meanwhile, a small amount of MgO can be found in this raw material. The main
source for Mg is the residual Mg used to prepare MgB$_2$. Mg vapor is generated during
the solid sintering of MgB$_2$ as the melting point of Mg (650 °C) is relatively low. To
fully react with B to form MgB$_2$, excess Mg is added during preparation. Residual
Mg, which acts as an impurity phase in MgB$_2$, is a main factor for the decrease in
T_C and the increase in ΔT [17–19]. Furthermore, the red curve is the R–T curve of
MgB$_2$ doped with 2.0 wt% Y$_2$O$_3$ prepared by the method in [29]. Results shows that
doping non-EL material Y$_2$O$_3$ decreases the superconducting transition temperature.

Figure 4 shows the R–T curves of MgB$_2$ doped with dopant A at concentrations of
0.5, 1.0, 1.5, 2.0, and 3.0 wt%. The corresponding samples are marked as S1, S2, S3,
S4, and S5. All the five curves clearly show the superconducting transition. When the
doping concentration is lower than 2 wt%, the resistivity values for the normal state
of the four samples are not obviously different. However, the increase in resistivity
value is large at a doping concentration of 3 wt%. All of the samples were pressed
into small pieces with a diameter of 12 mm and a thickness of 1 mm. The distance
among the four probes is 1 mm, and the resistance measurement of all of the samples
is under the same condition. Thus, the difference in normal resistance should not be
related to the variation of dimensions in the samples.

The onset temperature of these five samples is approximately 0.2 K lower than that
of pure MgB$_2$. Furthermore, the offset temperature of these samples is greatly affected
by the doping concentration, as shown in the inset of Fig. 4. The inset has listed three
measurements for the T_C^{off} of each sample. The abscissa of the inset image represents

Fig. 5 R–T curves for MgB$_2$ doping with dopants B, C, D, E, and F. Inset: corresponding T_C^{off} (Color figure online)
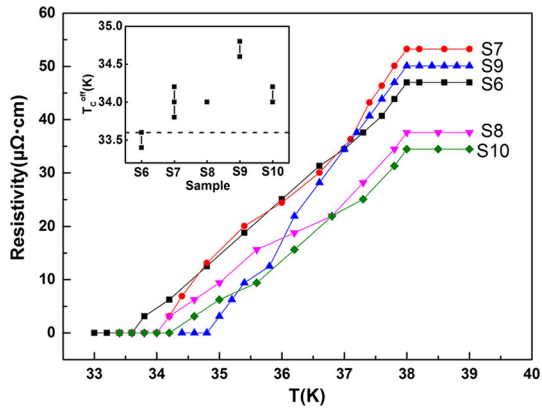
the five samples. The ordinate represents the value of T_C^{off}. It can be seen that some measurement results are overlapping and the measurement for T_C^{off} of all of the samples exhibited good reproducibility. The ordinate value of the dotted line in the inset image is 33.6 K, which is the T_C^{off} of pure MgB$_2$. The result shows that the value of T_C^{off} rises first and then decreases with the increase in doping concentration and most of the measurements are higher than that of pure MgB$_2$. When the doping concentration is 2.0 wt%, T_C^{off} is as high as 35.2 K, which is 1.6 K higher than that of pure MgB$_2$. The T_C^{off} of the other samples has also been improved by different degrees, except for S2, whose T_C^{off} is basically equal to that of pure MgB$_2$. The EL material YVO$_4$:Eu^{3+} is the only difference between the doped samples and pure MgB$_2$. Thus, the differences in T_C^{off} should be induced by the EL exciting effect of YVO$_4$:Eu^{3+} [29]. These results indicate that doping YVO$_4$:Eu^{3+} to MgB$_2$ is favorable to the improvement in T_C^{off}. Moreover, the optimum doping concentration is 2.0 wt%, which is consistent with the results of our previous works [28,29].

Figure 5 presents the R–T curves of the samples S6, S7, S8, S9, and S10. The multiple measurements for the offset temperature of each sample are presented in the inset image. The T_C^{off} of pure MgB$_2$ is also marked by dotted line. The doping concentrations of these five samples are all 2.0 wt% with different dopants, as shown in Table 2. The difference in resistivity values for the normal state of these samples is not obvious. The onset temperatures of all samples are all 38.0 K, which is 0.2 K lower than that of pure MgB$_2$. Except for S6, the offset temperatures of these samples are improved with different degree. The main reason for the difference in T_C^{off} is that these dopants have different thicknesses and EL intensities, which will result in a different EL exciting effect. The improvement in T_C^{off} is remarkable compared with MgB$_2$ doped with non-EL materials, such as Y$_2$O$_3$, because doping always decreases T_C. Similar results were described in our previous study [29], which revealed that T_C of MgB$_2$ doped with the EL material Y$_2$O$_3$:Eu^{3+} is 2.8 K higher than that of MgB$_2$ doped with Y$_2$O$_3$. Similar to the experimental results in Fig. 4, Fig. 5 indicates that doping EL materials into MgB$_2$ improves T_C^{off}.
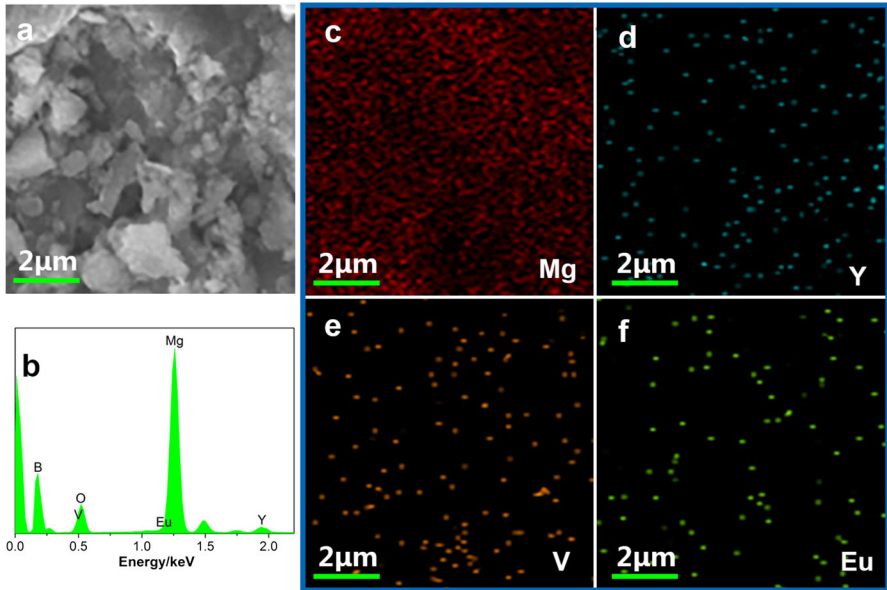
Fig. 6 SEM image of S4 (**a**), corresponding EDS (**b**), and EDS elemental mapping (**c–f**) (Color figure online)

The six kinds of dopants are all materials with good EL. During the R–T curve measurement, electrons would excite the dopants to generate EL, causing the EL exciting effect, which is favorable for the improvement in superconducting transition temperature [28,29]. However, as an impurity phase, the dopants would also introduce lattice defects and cause lattice distortion, which decreases the superconducting transition temperature. Thus, in order to improve the critical temperature as much as possible, the dopants should be uniformly dispersed in the sample to decrease the impurity effect and increase the EL exciting effect.

Figure 6a presents the SEM image for S4. Figure 6b shows the energy dispersive spectroscopy results. Mg, B, O, V, Y, and Eu, are detected in this sample. However, it is difficult to distinguish the inhomogeneous phase in the MgB_2 matrix from the SEM image; thus, EDS elemental mapping was chosen to display the dispersion of inhomogeneous phase. The distribution images of the metallic elements are presented in Fig. 6c–f. The corresponding element is listed in the lower right corner of each image. Lots of Mg conform to the XRD and energy dispersive spectroscopy results. Mg is uniformly dispersed throughout the image, which is not the same with the dispersion of V, Y, and Eu as shown in Fig. 6d–f. It can be seen that Fig. 6d–f is divided into many small black areas by V, Y, and Eu, respectively. These small areas consist of MgB_2 particles. Given that no chemical reaction occurred during sample preparation, the dispersion of the elements V, Y, and Eu can represent the dispersion of the dopants. Thus, Fig. 6d–f shows that the dopants are distributed around the MgB_2 particles to form a kind of superstructure the same with Fig. 1. Such a distribution is able to decrease the impurity effect and increase the EL exciting effect. The increase

in the offset temperature is attributed to the EL exciting effect induced by the dopants during resistivity measurement.

When the doping concentration is 2.0 wt%, different dopants exert different effects on the increase in T_C^{off}. If the dopant is A, the T_C^{off} is 35.2 K, which is 1.6 K higher than that of pure MgB_2. T_C^{off} will change to 33.6 K when dopant A is replaced with dopant B. Sample S4 has the highest offset temperature because the dopant A owns a strong EL intensity. Although dopant B also own a strong EL intensity, S6 does not have a high offset temperature because of the large thickness of dopant B, which is not conducive to inducing a strong EL exciting effect. In addition, the size and thickness of dopants C–F decrease in turn and their EL intensities increase in turn. The T_C^{off} of MgB_2 doped with dopants C, D, E, and F are 34.0, 34.0, 34.8, and 34.2 K, respectively. The results showed that the offset temperature of the samples doped with dopants C–F with same concentration does not strictly increase in turn. The main reason is that as the size and thickness decrease, the dopant flakes cannot be uniformly dispersed easily but are more likely to aggregate.

The effect of doping EL materials into MgB_2 on the superconductive transition temperature has been investigated in our previous study. At first, an in situ process has been applied to synthesize the samples [28]. The results showed that doping EL materials improves T_C. However, the dopant can react with boron to form YB_4 during the in situ process. Thus, an ex situ process was then applied to synthesize the samples to avoid such a reaction [29]. The results showed that the ex situ method can prevent the generation of YB_4. Meanwhile, the results confirmed that doping EL materials improves T_C. However, the improvement in T_C in our previous works is not obvious. In this study, we have systematically investigated the influence of the inhomogeneous phase on T_C and prepared the samples with higher superconducting transition temperature. Although, the superconducting transition width of 4.6 K is too large as for the pristine material, this experiment focuses on the change in T_C of the doped samples compared with that of pure MgB_2. Moreover, the raw materials of all samples are the same; thus the difference between these samples is the inhomogeneous phase, which is the inducing factor for different T_C. The result indicates that doping EL material favors the improvement in T_C^{off}. The largest improvement in T_C^{off} is 1.6 K. Actually, we have got the similar result even if the ΔT_C of pure MgB_2 is 1.8 K [29]. The large superconducting transition width should not change the experimental results. This study is also valuable in using commercial MgB_2.

5 Conclusion

The inhomogeneous phase of a smart meta-superconductor has a great effect on its superconductivity. In order to systematically investigate the influence of the inhomogeneous phase on T_C, six kinds of dopants with different sizes are prepared via the hydrothermal method. MgB_2-based meta-superconductors are prepared via a modified experimental method. EDS elemental mappings show that the inhomogeneous phases are comparatively uniformly dispersed around the MgB_2 particles; thus V, Y, and Eu were accumulated at a small area. The superconducting transition temperatures for the

samples are determined from the R–T curves, which are measured by the four-probe method. Results indicate that these six kinds of dopants have a different effect on the improvement in T_C^{off}. The optimum doping concentration is 2.0 wt%. Among all the samples, S4 doped with 2.0 wt% dopant A owns the highest T_C^{off}, which is 1.6 K higher than that of pure MgB$_2$. Although the mechanism that increases T_C^{off} remains to be clarified, the improvement in T_C^{off} is likely related to the size, thickness, and EL intensity of the inhomogeneous phase of the MgB$_2$ smart meta-superconductor. This experiment provides a novel approach for improving T_C and expands the practical application of superconducting materials.

References

1. J. Nagamatsu, N. Nakagawa, T. Muranaka, Y. Zenitani, J. Akimitsu, Nature **410**, 63–64 (2001)
2. C. Buzea, T. Yamashita, Supercond. Sci. Technol. **14**, R115–R146 (2001)
3. J.S. Slusky, N. Rogado, K.A. Regan, M.A. Hayward, P. Khalifah, T. He, K. Inumaru, S.M. Loureiro, M.K. Haas, H.W. Zandbergen, R.J. Cava, Nature **410**(6826), 343–345 (2001)
4. H. Luo, C.M. Li, H.M. Luo, S.Y. Ding, J. Appl. Phys. **91**(10), 7122–7124 (2002)
5. R.J. Cava, H.W. Zandbergen, K. Inumaru, Physica C **385**, 8–15 (2003)
6. S.M. Kazakov, R. Puzniak, K. Rogacki, A.V. Mironov, N.D. Zhigadlo, J. Jun, C. Soltmann, B. Batlogg, J. Karpinski, Phys. Rev. B **71**(2), 024533 (2005)
7. A. Bianconi, Y. Busby, M. Fratini, V. Palmisano, L. Simonelli, M. Filippi, S. Sanna, F. Congiu, A. Saccone, M. Giovannini, S. De Negri, J. Supercond. Nov. Magn. **20**(7), 495–501 (2007)
8. O. de la Peña, A. Aguayo, R. de Coss, Phys. Rev. B **66**(1), 012511 (2002)
9. J. Kortus, O.V. Dolgov, R.K. Kremer, A.A. Golubov, Phys. Rev. Lett. **94**(2), 027002 (2005)
10. Y.G. Zhao, X.P. Zhang, P.T. Qiao, H.T. Zhang, S.L. Jia, B.S. Cao, M.H. Zhu, Z.H. Han, X.L. Wang, B.L. Gu, Physica C **361**, 91–94 (2001)
11. M. Monni, M. Affronte, C. Bernini, D. Di Castro, C. Ferdeghini, M. Lavagnini, P. Manfrinetti, A. Orecchini, A. Palenzona, C. Petrillo, P. Postorino, A. Sacchetti, F. Sacchetti, M. Putti, Physica C **460–462**, 598–599 (2007)
12. A.V. Sologubenko, N.D. Zhigadlo, S.M. Kazakov, J. Karpinski, H.R. Ott, Phys. Rev. B **71**(2), 020501 (2005)
13. K. Rogacki, B. Batlogg, J. Karpinski, N.D. Zhigadlo, G. Schuck, S.M. Kazakov, P. Wägli, R. Puźniak, A. Wiśniewski, F. Carbone, A. Brinkman, D. van der Marel, Phys. Rev. B **73**(17), 174520 (2006)
14. A.V. Sologubenko, N.D. Zhigadlo, J. Karpinski, H.R. Ott, Phys. Rev. B **74**(18), 184523 (2006)
15. S.X. Dou, S. Soltanian, J. Horvat, X.L. Wang, S.H. Zhou, M. Ionescu, H.K. Liu, P. Munroe, M. Tomsic, Appl. Phys. Lett. **81**(18), 3419–3421 (2002)
16. J.H. Kim, S. Zhou, M.S.A. Hossain, A.V. Pan, S.X. Dou, Appl. Phys. Lett. **89**(14), 142505 (2006)
17. P. Postorino, A. Congeduti, P. Dore, A. Nucara, A. Bianconi, D. Di Castro, S. De Negri, A. Saccone, Phys. Rev. B **65**(2), 020507 (2001)
18. T. Takenobu, T. Ito, D. Hieu Chi, K. Prassides, Y. Iwasa, Phys. Rev. B **64**(13), 134513 (2001)
19. A. Bianconi, S. Agrestini, D. Di Castro, G. Campi, G. Zangari, N.L. Saini, A. Saccone, S. De Negri, M. Giovannini, G. Profeta, A. Continenza, G. Satta, S. Massidda, A. Cassetta, A. Pifferi, M. Colapietro, Phys. Rev. B **65**(17), 174515 (2002)
20. J.Q. Li, L. Li, F.M. Liu, C. Dong, J.Y. Xiang, Z.X. Zhao, Phys. Rev. B **65**(13), 134426 (2002)
21. W. Mickelson, J. Cumings, W.Q. Han, A. Zettl, Phys. Rev. B **65**(5), 052505 (2002)
22. R.H. Wilke, S.L. Bud'ko, P.C. Canfield, D.K. Finnemore, R.J. Suplinskas, S.T. Hannahs, Phys. Rev. Lett. **92**(21), 217003 (2004)
23. H. Liu, X.P. Zhao, Y. Yang, Q.W. Li, J. Lv, Adv. Mater. **20**(11), 2050–2054 (2008)
24. Y.P. Qiao, X.P. Zhao, Y.Y. Su, J. Mater. Chem. **21**(2), 394–399 (2011)

25. X.P. Zhao, J. Mater. Chem. **22**(19), 9439–9449 (2012)
26. W.T. Jiang, Z.L. Xu, Z. Chen, X.P. Zhao, J. Funct. Mater **38**, 157–160 (2007) (**in Chinese**). http://www.cnki.com.cn/Article/CJFDTOTAL-GNCL200701046.htm
27. S.H. Xu, Y.W. Zhou, X.P. Zhao, Mater. Rev. **21**, 162–166 (2007) (**in Chinese**). http://www.cnki.com.cn/Article/CJFDTotal-CLDB2007S3048.htm
28. Z.W. Zhang, S. Tao, G.W. Chen, X.P. Zhao, J. Supercond. Nov. Magn. **29**(5), 1159–1162 (2016)
29. S. Tao, Y.B. Li, G.W. Chen, X.P. Zhao, J. Supercond. Nov. Magn. **30**(6), 1405–1411 (2017)
30. D.A. Kirzhnits, E.G. Maksimov, D.I. Khomskii, J. Low Temp. Phys. **10**(1–2), 79–93 (1973)
31. I.I. Smolyaninov, V.N. Smolyaninova, Adv. Condens. Matter Phys. **91**(9), 479635 (2014)
32. V.N. Smolyaninova, B. Yost, K. Zander, M.S. Osofsky, H. Kim, S. Saha, R.L. Greene, I.I. Smolyaninov, Sci. Rep. **4**, 7321 (2014)
33. V.N. Smolyaninova, K. Zander, T. Gresock, C. Jensen, J.C. Prestigiacomo, M.S. Osofsky, I.I. Smolyaninov, Sci. Rep. **5**, 15777 (2015)
34. W.C. Qi, G.W. Chen, C.S. Yang, C.R. Luo, X.P. Zhao, J. Mater. Sci.: Mater. Electron. **28**(13), 9237–9244 (2017)